CrossMark

ORIGINAL CONTRIBUTION

Viscoelasticity and morphology of polystyrene-*block*-poly[ethylene-co-(ethylene-propylene)]-*block*-polystyrene tri-block copolymer/paraffinic oil blends. 1. Effect of oil content

Yuji Aoki[1] · Ryohei Takahashi[1] · Shotaro Nishitsuji[1] · Akira Ishigami[1] · Tomonori Koda[1] · Akihiro Nishioka[1]

Abstract We have investigated the microdomain structure and viscoelastic properties of polystyrene-*block*-poly(ethylene-co-(ethylene-propylene)-*block*-polystyrene copolymer (SEEPS-1)/paraffinic oil (Oil-1) blends. The SAXS results revealed that, with increasing oil content, the structures change from a lammelar microdomain for SEEPS-1/Oil-1 = 100/0 to a hexagonally packed cylindrical microdomain for SEEPS-1/Oil-1 = 75/25 blend, and furthermore change to a spherical microdomain packed in a cubic lattice for SEEPS-1/Oil-1 = 50/50 and 25/75 blends. SEEPS-1/Oil-1 = 100/0 and 75/25 blends held each same microdomain structure below 300 °C. In contrast, SEEPS-1/Oil-1 = 50/50 and 25/75 blends, respectively, exhibited order-disorder transition temperature (T_{ODT}) at 210–220 °C and 150–160 °C. Below T_{ODT}, the microdomain structures did not change. Corresponding to the SAXS observations, the viscoelastic responses showed that the dynamic storage modulus G', respectively, is proportional to $\omega^{1/2}$, $\omega^{1/4} \sim \omega^{1/3}$, and ω^0 at low frequencies for SEEPS-1/Oil-1 = 100/0, 75/25, and 50/50 and 25/75, indicating lamellar, cylindrical, and spherical microdomains The time-temperature superposition was applicable on the ordered state, and the activation energy obtained from the shift factors was roughly independent of blend composition (in other words, microdomain structure), suggesting that the viscoelastic responses are due to the presence of defects of long range order of microdomain structures.

Introduction

It is well-known that block copolymers have the ordered microphase-separated structure in the form of spheres, cylinders, lamellae, or bicontinuous microdomains. However, as the temperature is raised above a certain critical value, the microphase-separated structure disappears, giving rise to a disordered state. Such a phenomenon is referred to as the order-disorder transition (ODT). The microdomain structure affects the viscoelastic properties on time scales longer than the single-chain terminal relaxation time (τ_c). It has been a great deal of interest in correlating the rheological properties of block copolymers with the microdomain structures (Fredrickson and Bates 1996). Gouinlock and Porter (1977) and Chung and Lin (1978) first demonstrated that the low-frequency viscoelastic properties of SBS triblock copolymer was dependent on the state of order. Viscoelastic properties at the low frequency ($\omega < \omega_c \approx 0.1\tau_c^{-1}$) are strongly dependent on the type of microdomain structure below the ODT temperature (T_{ODT}).

Block copolymer melts are easily trapped in morphologies with local compositional order but macroscopic (long-range) isotropy. Such polycrystalline morphologies are inevitable in samples that have been prepared by compounding or solvent casting. Certain types of defects (dislocations, grain boundaries, etc.) can be difficult to remove. It is important to recognize that the linear viscoelastic response can be quite sensitive to the degree of long-range order in a block copolymer melt,

✉ Yuji Aoki
y.aoki@yz.yamagata-u.ac.jp

[1] Graduate School of Science and Engineering, Yamagata University, 4-3-16, Jonan, Yonezawa, Yamagata 992-8510, Japan

🖄 Springer

particularly at low and intermediate frequencies (Koppi et al. 1992; Larson et al. 1993).

Experimentally, it has been found that the dynamic storage modulus G' and loss modulus G'' of lamellar microdomain structures are proportional to $\omega^{1/2}$ at low frequencies (Bates 1984; Rosedale and Bates 1990; Patel et al. 1995; Wang et al. 1999; Floudas et al. 1999). For cylindrical microdomain structures, $G' \propto \omega^{1/3} \sim \omega^{1/6}$ were found (Morrison and Winter 1989; Morirson et al. 1990; Winter et al. 1993; Balsara et al. 1996; Ryu et al. 1997). Cubic microdomain structures exhibit solid-like behavior ($G' \sim \omega^0$) over a wide range of frequencies (Watanabe et al. 1982; Koppi et al. 1994; Kossuth et al. 1999). Theoretically, the linear viscoelasticity of quenched block copolymer lamellar phases with local uniaxial order and global isotropy has been studied by Kawasaki and Onuki (1990). They argued for a mesoscopic origin of the unusual power law scaling ($\sim \omega^{1/2}$) of G' and G''. Rubinstein and Obukhov (1993) argued that the stress relaxation modulus $G(t)$ is proportional to $t^{-1/2}$ for quenched lamellae, consistent with Kawasaki and Onuki scalings of the dynamic moduli, and $t^{-1/4}$ for quenched cylinder. However, the relations between the microdomain structures and the viscoelastic properties of block copolymers have not been fully elucidated.

Paraffinic oils are often used to improve the rigidity and processability of thermoplastic elastomers consisting of block copolymers. Mortensen et al. (1998, 2002) studied the structure and rheology of SEBS/paraffinic oil blends. They found that the PEB midblock is dissolved in the paraffinic oil and the micellar network structure are formed. Sugimoto et al. (2009) studied the effect of paraffinic oil on the rheological and phase behaviors of SEBS/oil blend. Due to the small polarity difference between the elastomer phase and oil, the oils are present in the elastomer phase, and thus lower the T_{ODT}. However, the effect of paraffinic oil on the microdomain structures and the low-frequency viscoelastic properties has been less studied.

Recently, we prepared a series of blend systems of polystyrene-block-poly(ethylene-co-ethylene-propylene)-block-polystyrene (SEEPS) and three kinds of paraffinic oil having different molecular weights (MWs) and studied their dynamic viscoelastic properties at the solid state (Nishioka et al. 2011) and at the molten state (Takahashi et al. 2012). We found that paraffinic oil is a selective solvent to poly(ethylene-co-(ethylene-propylene) (PEEP) midblock (elastomer phase) and is mainly dissolved into the phase. We determined their T_{ODT} for the SEEPS/oil blends with three kinds of oil using two rheological methods and found that the viscoelastic properties and ODT behavior of the blends depended strongly on the oil MW, because of the difference of solubility of paraffinic oil to the PS phase.

In this paper, we have investigated the microdomain structure and viscoelastic properties of SEEPS/paraffinic oil blends. We found that, with increasing oil content, the structures change from a lammelar microdomain to a hexagonally packed cylindrical microdomain, and furthermore change to a spherical microdomain packed in a cubic lattice. Corresponding to these microdomain structures, the viscoelastic properties exhibited different power law behavior at low frequencies. The relation between the microdomain structure and the temperature dependence of the viscoelastic properties at low frequencies is also discussed. Details of these results are presented in this paper.

Experimental methods

The material used was a commercial SEEPS tri-block copolymer (SEPTON-4033, Kuraray Co. Ltd., Japan) and was designated SEEPS-1. The molecular weight of SEEPS-1 was determined by gel permeation chromatography (GPC) using PS elution standards. The total weight-average molecular weight M_w of SEEPS-1 was 84 kg/mol, and the weight fraction of the PS block was 0.30. A Diana Process Oil (PW-380, Idemitsu Kosan Co. Ltd., Japan) was used and designated Oil-1. Oil-1 is a mixture of saturated hydrocarbons consisting of about 70 wt.% of paraffinic and 30 wt.% of naphthenic components and possesses average molecular weights of 750 g/mol, according to the sample provider.

SEEPS-1 and Oil-1 were mixed as a dry blend and left for about 20 h at room temperature. Then, the mixtures were blended by a twin-screw extruder (model: ULT nano, Technovel Co. Ltd., Japan) at 100 rpm for about 10 min. Blending temperature was 240 °C for SEEPS-1/Oil-1 = 100/0 and SEEPS-1/Oil-1 = 75/25 and 180 °C for SEEPS-1/Oil-1 = 50/50 and SEEPS-1/Oil-1 = 25/75. Blended samples were subsequently compression molded into a disk shape (1-mm thickness, 25 or 50 mm φ) at 180 °C and 5 MPa for 10 min by a Mini Test Press-10 (Toyo Seiki Seisakusho Co., Ltd., Japan).

SAXS measurements were conducted using X-ray diffraction apparatus (NANO-Viewer, Rigaku, Japan). The incident X-ray beam was generated from a Cu-Kα line (wavelength $\lambda = 1.54$ A) and was focused to a spot 450 μm in diameter at the sample position with a confocal optic (Max-Flux, Rigaku, Japan) equipped with a pinhole slit collimator. The scattered X-ray from the sample were detected by a two-dimensional position-sensitive detector (Pilatus 100K/R, Rigaku, Japan), with 195 × 487 pixels (33.5 × 83.8 mm) and a spatial resolution of 0.172 mm, covering a q range of (0.02 A^{-1} < q < 0.5 A^{-1}) at a sample-to-detector distance of 325 mm. The scattering data recorded on the detector were corrected for counting efficiency, instrumental background, and air scattering on a pixel-to-pixel basis. The scattering intensity distribution $I(q)$ was circular averaged. Temperature was controlled to within ±1 °C using a FP900 Thermosystem (Mettler Toledo).

Dynamic viscoelastic measurements were performed on a stress control rheometer (Physica MCR-300, Anton Paar)

operated in the parallel plate geometry with 25-mm diameter and about 1-mm gap. The dynamic storage modulus (G') and loss modulus (G'') were obtained as a function of angular frequency (ω). The G' and G'' were measured at different temperatures in order to investigate the temperature dependence of the viscoelastic properties. Strain amplitude of 0.7 % was used for samples below T_{ODT} and 7 % for samples above T_{ODT}. These small amplitudes are low enough to lie within the linear range. The time-temperature superposition (Ferry 1980) was applicable below or above T_{ODT}, and the G' and G'' data were superimposed onto the master curves. Then, the data could be obtained over a wide frequency range. All experiments were performed under nitrogen atmosphere so as to minimize oxidative degradation at high temperatures.

Results and discussion

SAXS study

The SAXS patterns for SEEPS-1/Oil-1 = 100/0, 75/25, 50/50, and 25/75 samples exhibited azimuthally isotropic rings. Figure 1 shows the SAXS profiles for the four samples at room temperature, where q is the magnitude of scattering vector defined by $q = (4\pi/\lambda) \sin(\theta/2)$ with λ and θ being the
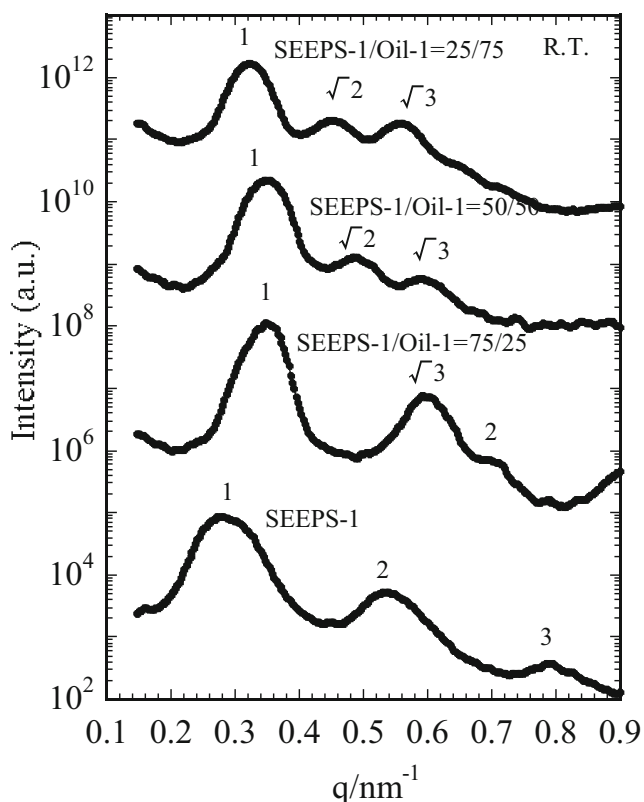
wavelength of X-ray and scattering angle, respectively. The number on the peaks in the figure represents the spacing ratio. To avoid overlaps of the SAXS profiles, these are vertically shifted. The following observations can be seen in Fig. 1.

1. The ratio of peak position is 1:2:3 for SEEPS-1/Oil-1 = 100/0, indicating that this sample has a lamellae microdomain structure.
2. The ratio of peak position is 1:√3:2 for SEEPS-1/Oil-1 = 75:25, indicating that this oil blend has a hexagonally-packed cylindrical microdomain structure of polystyrene block.
3. The ratio of peak position for SEEPS-1/Oil-1 = 50/50 and 25/75 is 1:√2:√3, indicating that these oil blends have a spherical microdomain packed in a cubic lattice (Sakamoto et al. 1997).

These SAXS observations indicate that the samples obtained blended by an extruder are locally ordered but macroscopically disordered (i.e., globally isotropic) states.
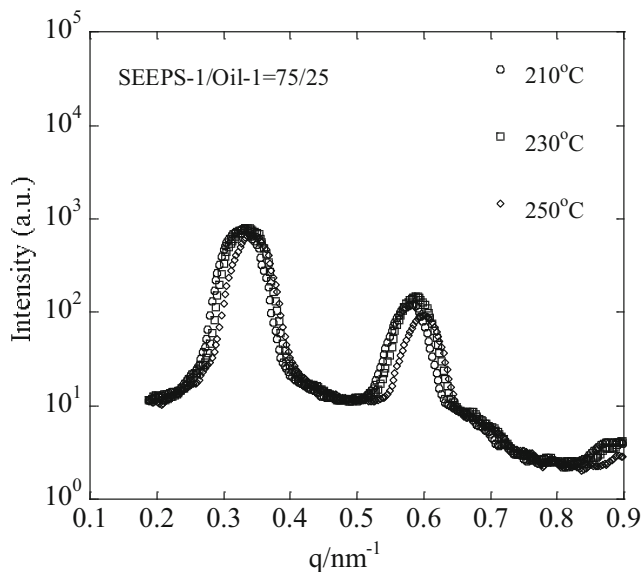
For a pure ABA triblock copolymer, the microdomain structure is most strongly affected by the total volume fraction f_A of blocks A. For roughly equal amounts of A and B, lamellae form. If f_A is smaller than 0.3–0.35, then cylinders of A usually form. If $f_A \leq 0.18$–0.23, spheres of A form in a matrix of B (Larson 1999). We can roughly estimate the volume fraction of PS blocks in SEEPS-1/Oil-1 blends, using the density of 1.0, 0.9, and 0.9 g/cm³, respectively, for PS, elastomer (PEEP), and Oil-1. For SEEPS-1/Oil-1 = 100/0, the volume fraction of PS blocks is obtained to be around 0.28. We suppose that SEEPS-1/Oil-1 = 100/0 is a boundary between lamellae and cylinder, although this sample has a lamellae microdomain, as shown from SAXS observations, and the volume fraction is somewhat smaller than that of lamellae previously reported for ABA triblock copolymers. Paraffinic oil (Oil-1) is a selective solvent to the elastomer phase (PEEP) and Oil-1 dissolves in the PEEP (Nishioka et al. 2011). Then, the matrix phase is a mixture of PEEP and Oil-1. Using these densities, the volume fraction was obtained to be 0.17, 0.14, and 0.07, respectively, for SEEPS-1/Oil-1 = 75/25, 50/50, and 25/75 blends. The microdomain structure of SEEPS-1/Oil-1 blends is very similar to the phase diagrams for a pure AB and ABA block copolymer reported by Larson (1999), although each microdomain structure shifts to slightly lower volume fraction.

Figures 2, 3, 4, and 5, respectively, show the SAXS profiles for SEEPS-1/Oil-1 = 100/0, 75/25, 50/50, and 25/75 blends at various temperatures as the temperature was increased. The microdomain structures of SEEPS-1/Oil-1 = 100/0 and 75/25 did not change at elevating temperature, as the peak position hardly changed with
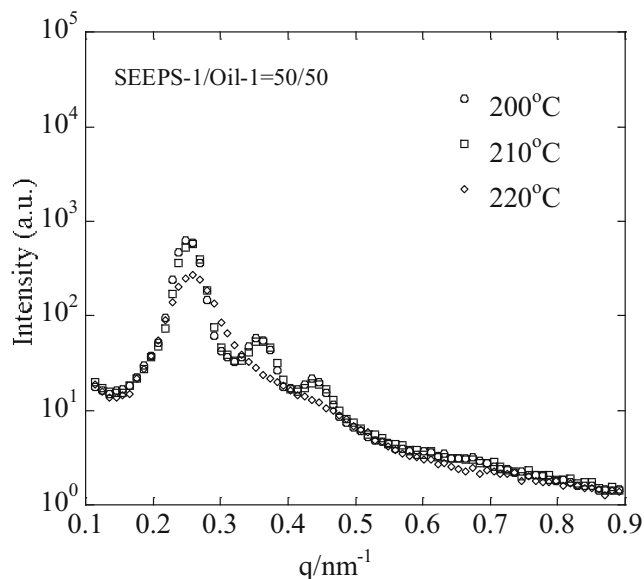

Fig. 1 SAXS profiles measured at room temperature for SEEPS-1/Oil-1 = 100/0, 75/25, 50/50, and 25/75 blends
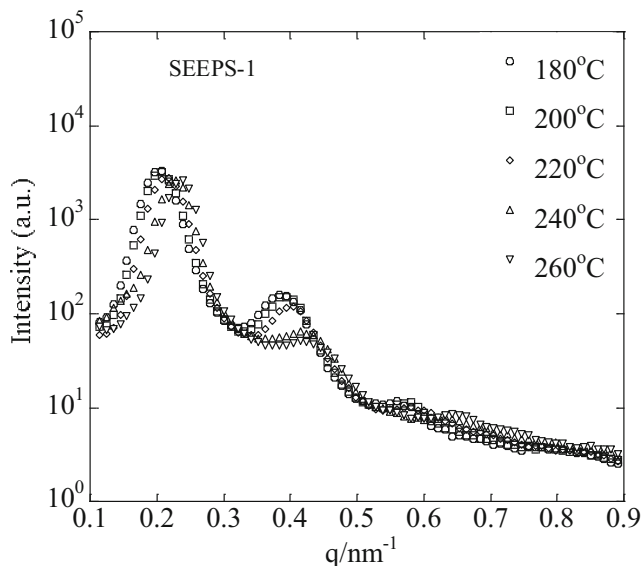
Fig. 2 SAXS profiles for SEEPS-1 (SEEPS-1/Oil-1 = 100/0) at various temperatures as indicated

Fig. 4 SAXS profiles for SEEPS-1/Oil-1 = 50/50 blend at various temperatures as indicated

temperature up to about 220 °C although slightly shifted to a larger q value above 240 °C. This shift is due to the small change of the lamellar domain structure because the ratio of peak position was the same. On the other hand, the structure of SEEPS-1/Oil-1 = 50/50 and 25/75 blends, respectively, suddenly changed as the temperature increases from 210 to 220 °C and 150 to 160 °C. These changes indicate that order-disorder transition (ODT) took place at 210–220 °C for the 50/50 blend and 150–160 °C for the 25/75 blend. A detailed analysis of SAXS profiles of the blends will be presented in a separate paper.

Viscoelastic properties

The G' and G'' versus ω curves at various temperatures T were superimposed into a master curve by shift along the ω axis by a factor a_T. Figure 6 shows the master curves of G' and G'' for SEEPS-1/Oil-1 = 100/0 at 0.7 % strain. We can find that the G'' data could be excellently superimposed into the master curve, although the G' data are somewhat noisy at low frequencies. Both G' and G'' display weak frequency dependencies over the entire frequency range up to the maximum temperature investigated, implying that T_{ODT} exceeds 300 °C,

Fig. 3 SAXS profiles for SEEPS-1/Oil-1 = 75/25 blend at various temperatures as indicated
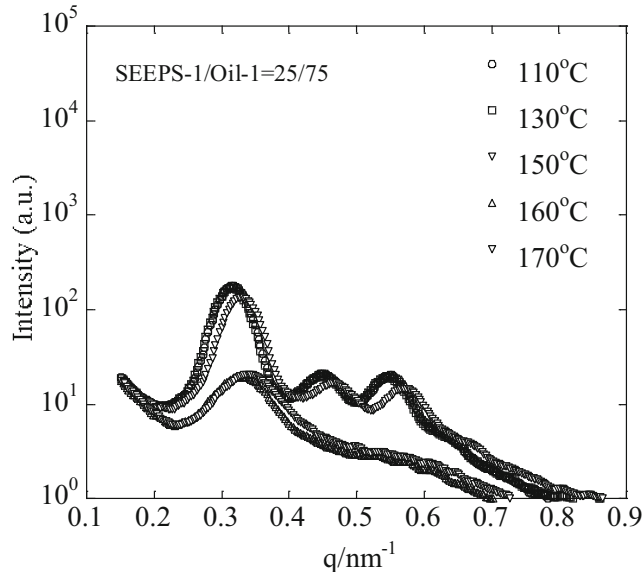
Fig. 5 SAXS profiles for SEEPS-1/Oil-1 = 25/75 blend at various temperatures as indicated
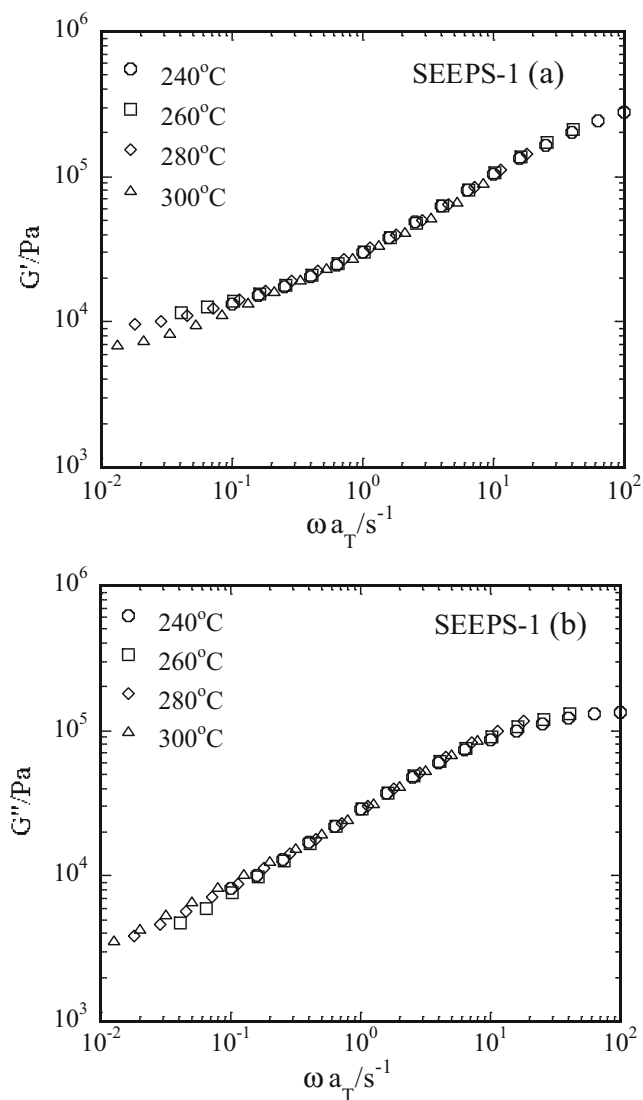
Fig. 6 Master curves of the storage modulus G′ (**a**) and loss modulus G″ (**b**) for SEEPS-1. The reference temperature is 240 °C
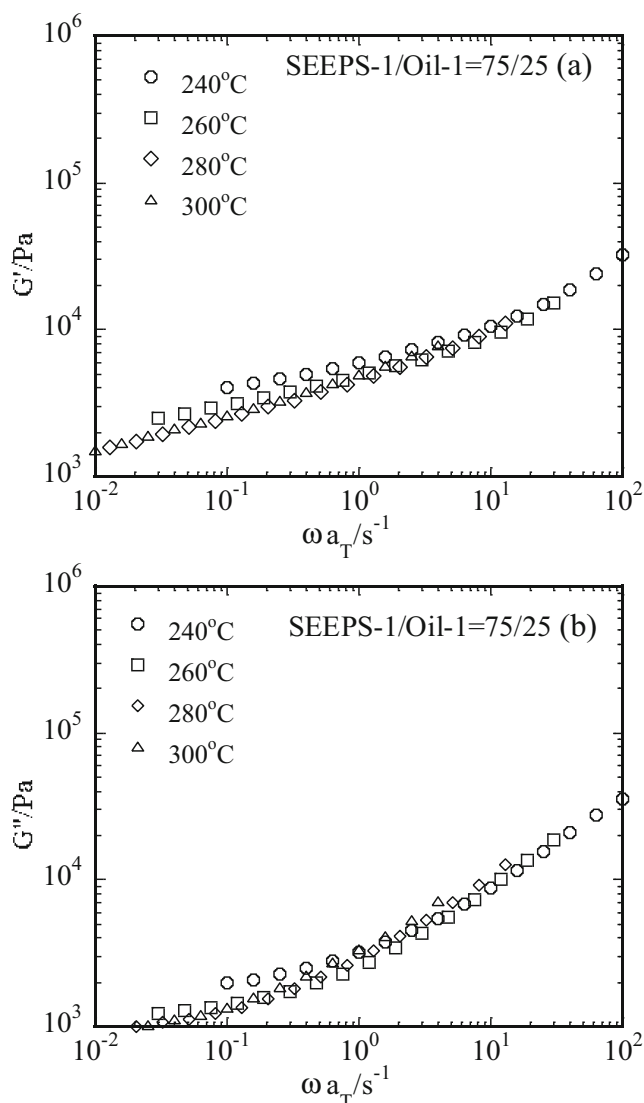
microdomain with locally uniaxial order and global isotropy. Our sample is considered to have the structure close to "perfect" isotropy because the G′ and G″ data exhibit the low-frequency power laws. However, the G′ data seem to level off at low frequencies. This may be due to imperfect isotropy.

For SEEPS-1/Oil-1 = 100/0, we did not measure the viscoelastic properties above 300 °C, because degradation severely occurred. We could not observe the order-disorder transition in this T range by viscoelastic measurements, too. Degradation occurred before T_{ODT} is reached, as the total MW of SEEPS-1 is high.

Figure 7 shows the master curves of SEEPS-1/Oil-1 = 75/25 blend at 0.7 % strain. We can find that time-temperature superposition holds well, although some scatterings in G′ and G″ were found comparing with those of SEEPS-1/Oil-

because the terminal behavior of G′ and G″, G′ ∝ ω^2, and G″ ∝ ω, was not be observed. Interestingly, Fig. 6 shows that the G′ and G″ exhibited a power law behavior of G′ and G″ ∝ $\omega^{1/2}$ between $10^{-1} < \omega a_T < 10^1$.

The low-frequency viscoelastic properties are strongly dependent on the type of microdomain structure below T_{ODT}. The most intensively studied morphology is the lamellar microdomain, where $G' \approx G'' \sim \omega^{1/2}$ at low frequencies (Bates 1984; Rosedale and Bates 1990; Kawasaki and Onuki 1990; Rubinstein and Obukhof 1993; Patel et al. 1995; Wang et al. 1999; Floudas et al. 1999). The SAXS observation revealed that SEEPS-1/Oil-1 = 100/0 has a lamellar microdomain structure. Our data are in good agreement with the power law index of 1/2 for lamellar microdomains. Thus, we can conclude that SEEPS-1/Oil-1 = 100/0 has the lamellar microdomains. The power law index is an averaged value for lamellar

Fig. 7 Master curves of the storage modulus G′ (**a**) and loss modulus G″ (**b**) for SEEPS-1/Oil-1 = 75/25 blend. The reference temperature is 240 °C

1 = 100/0. Here, values of a_T were chosen that both G' and G'' were best satisfied. SEEPS-1/Oil-1 = 75/25 blend did not show the terminal flow behavior and displayed rheological behavior characteristic of microscopically ordered materials over the entirely experimental T window, indicating $T_{ODT} > 300\ °C$ for the blend. Thus, the blend is also microphase separated and exhibit viscoelastic properties unlike those of homopolymer melts. The G' behavior at low ω characterizes the blend which exhibits a power law behavior of $G' \propto \omega^n$, where n is about 1/4~1/3. This n value is smaller than that for SEEPS-1/Oil-1 = 100/0 blend. The SAXS measurements indicate that SEEPS-1/Oil-1 = 75/25 blend has a hexagonally packed cylindrical microdomain structure of polystyrene block. For cylindrical microdomain structures, $G' \propto \omega^{1/3} \sim \omega^{1/6}$ were found (Morrison and Winter 1989; Morrison et al. 1990; Rubinstein and Obukhof 1993; Winter

et al. 1993; Balsara et al. 1996; Ryu et al. 1997). Our n value is in good agreement with the power law index of 1/3~1/6 for cylindrical domains.

Figure 8 shows the master curves of G' (a) and G'' (b) for SEEPS-1/Oil-1 = 50/50 blend below and above T_{ODT}. Here, open symbols indicate the data below T_{ODT} measured at 0.7 % strain and filled symbols above T_{ODT} measured at 7 % strain at a reference temperature of 210 °C. The data have been shifted along ω axis using the shift factors of the G'' data, as the G'' data could be superimposed at high ω, because G'' is less sensitive to the phase transition. This method of time-temperature shifting, whereby superposition of the high ω data is achieved, is the same as that used by Koppe et al. (1992) and Patel et al. (1995). We can find that both G' and G'' data could be superimposed into each master curve below and above T_{ODT}, although the G'' data just below T_{ODT} at low frequencies were a little scattered.

Above T_{ODT}, both G' and G'' show liquid-like terminal behavior at low ω: $G' \propto \omega^2$ and $G'' \propto \omega$, typically observed for flexible polymers. For SEEPS-1/Oil-1 = 50/50 blend, the longest relaxation time is very short above T_{ODT}, and the terminal region is observed at the entire ω range. Below T_{ODT}, on the other hand, the following observations are worth noting in the low ω zone of Fig. 8. The plots of log G' versus log ω show very weak ω dependence and the G' values are constant at low ω. This rheological response is governed by the spherical microdomains of PS, as already shown for SEBS/oil = 50/50 blend by Sugimoto et al. (2009) and explained in the "Introduction": cubic microdomain structure exhibits solid-like behavior ($G' \sim \omega^0$) over a wide range of frequencies (Watanabe et al. 1982; Koppi et al. 1994; Kossuth et al. 1999).

Figure 8 indicates that SEEPS-1/Oil-1 = 50/50 blend reached the disorder state at 220 °C and T_{ODT} of this blend is determined to be between 210 and 220 °C. A sudden displacement at 220 °C in the plots of G' versus log ω, but no sudden displacement is observed in the plots of log G'' versus log ω. This observation seems to indicate that G', which describes the elastic properties, is much more sensitive to a change in phase morphology of block copolymer/oil blend systems at a certain critical T than G'', which describes the viscous properties.

Figure 9 shows the master curves of G' (a) and G'' (b) for SEEPS-1/Oil-1 = 25/75 blend below and above T_{ODT}. Here, open symbols indicate the data below T_{ODT} at 0.7 % strain and filled symbols above T_{ODT} at 7 % strain at the reference temperature of 150 °C. The master curves of the blend were constructed as same as those of the 50/50 blend. The G' and G'' data are very similar to those of the 50/50 blend below and above T_{ODT}, although the T_{ODT} (between 150 and 160 °C) and the G' value (3.5×10^3 Pa for the 25/75 blend and 8×10^3 Pa for the 50/50 blend) of the 25/75 blend, are lower than those of
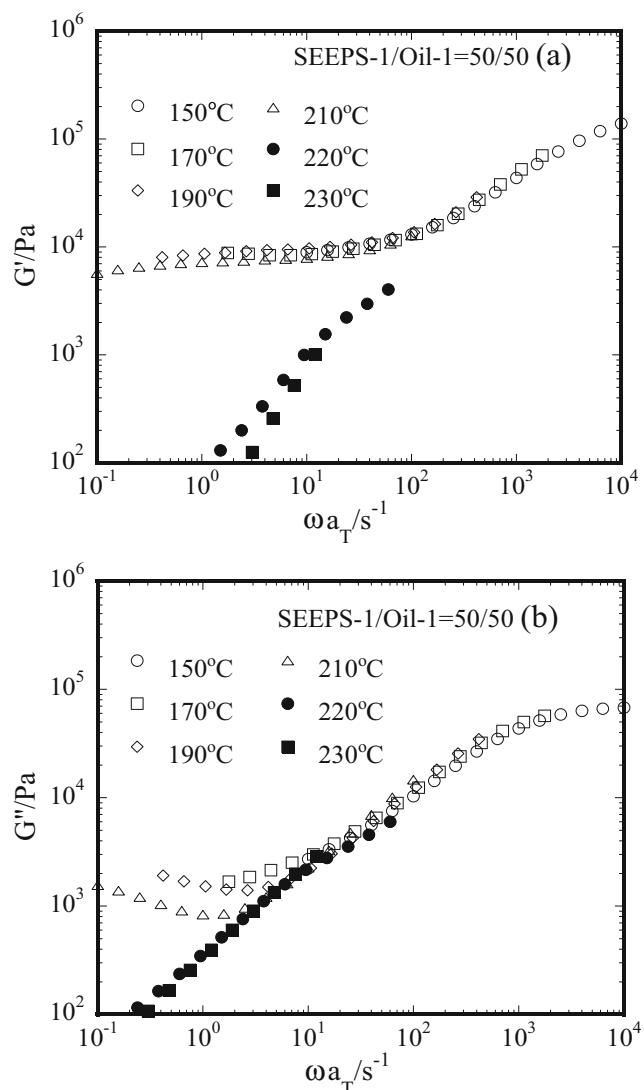
Fig. 8 Master curves of the storage modulus G' (a) and loss modulus G'' (b) for SEEPS-1/Oil-1 = 50/50 blend. The reference temperature is 210 °C
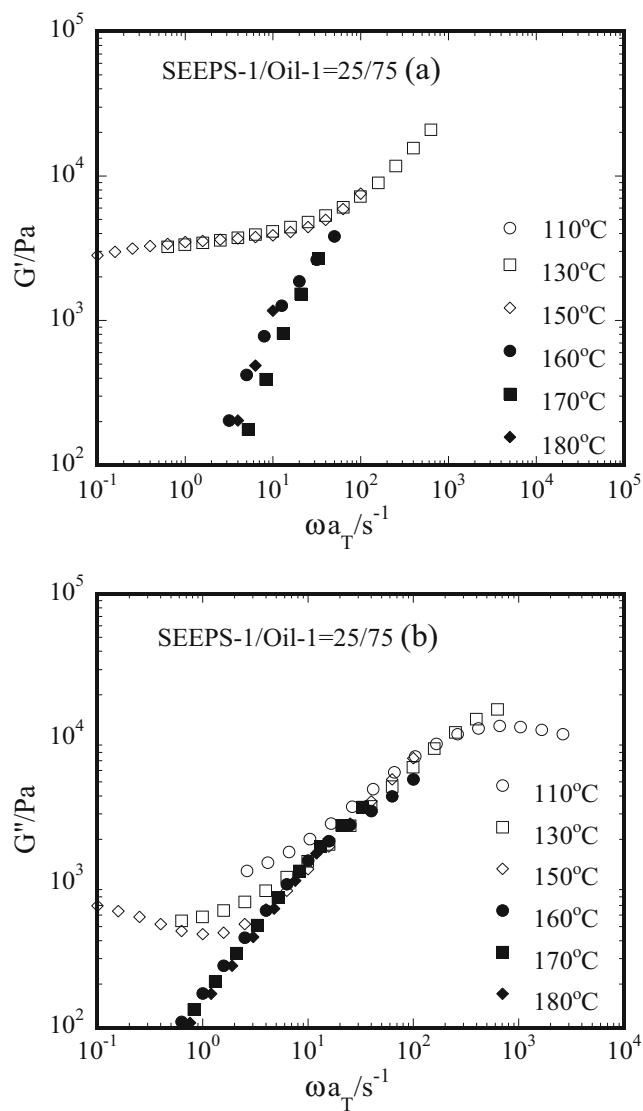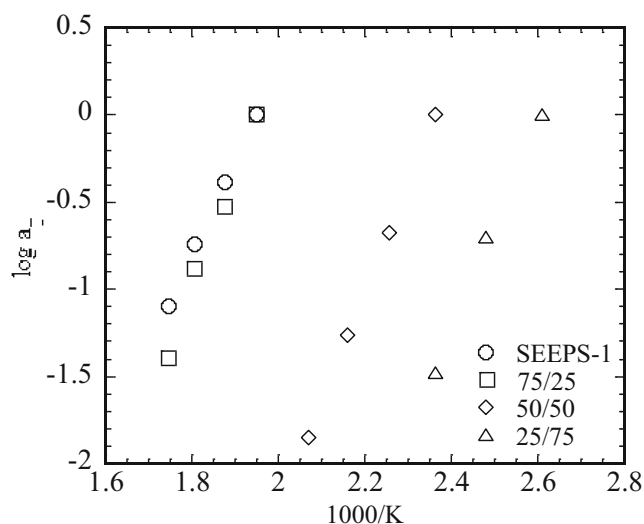
Fig. 9 Master curves of the storage modulus G′ (**a**) and loss modulus G″ (**b**) for SEEPS-1/Oil-1 = 25/75 blend. The reference temperature is 150 °C

Fig. 10 Shift factor a_T plotted against reciprocal temperature for SEEPS-1/Oil-1 = 100/0, 75/25, 50/50, and 25/75 blends

the 50/50 blend. Solid-like behavior ($G' \sim \omega^0$) was found at low frequencies below T_{ODT}, as expected by SAXS measurements, and terminal flow behavior was found above T_{ODT}.

Shift factor

Temperature dependence of the viscoelastic properties for block copolymers were reported in several papers (Gouinlock and Porter 1977; Chung and Lin 1978; Morrison et al. 1990; Rosedale and Bates 1990; Winter et al. 1993; Patel et al. 1995). Chung and Lin (1978) studied the rheological properties of SBS block copolymer and found that the shift factor was represented by Arrhenius-type activation energy ΔE ($\Delta E \approx 100$ kJ/mol).

Figure 10 shows the shift factor a_T versus inverse temperature $1000/T$ for SEEPS-1/Oil-1 = 100/0, 75/25, 50/50, and 25/75

blends below T_{ODT}, in other words, in the ordered state. It was found that the T dependence of the shift factor a_T obeys the time-temperature superposition with the Arrhenius-type activation energy ΔE, indicating that the morphology did not change at elevating T. From the slope of these plots, the activation energy ΔE was calculated and listed in Table 1. The ΔE values are similar to that obtained by Chung and Lin (1978) and are almost the same irrespective of blend ratio. It is surprising, and perhaps partially fortuitous, ΔE values are independent of oil concentration. What mechanism governs the ΔE behavior?

When the ΔE values of SEEPS-1/Oil-1 blends are due to the relaxation of individual chains, the ΔE of SEEPS-1/Oil-1 = 25/75 blend should be different from that of the 50/50 blend, as both blends have a sphere morphology in the ordered state. Then, the matrix phase in the locally ordered spherical microdomains is consisted of PEEP/oil blend. As we reported previously (Nishioka et al. 2011), paraffinic oil is a selective solvent to the elastomer phase (PEEP) in SEEPS tri-block copolymer and mainly dissolved in the elastomer phase. For SEEPS-1/Oil-1 = 25/75 blend, segregation of PS block chains and PEEP block chains with Oil-1 is strongly, as Oil-1 hardly dissolve into PS. Then, the PEEP concentration (41 wt.%) of SEEPS-1/Oil-1 = 50/50 blend is two times higher than that (19 wt.%) of 25/75 blend. For concentrated polymer solutions, ΔE value decreases with increasing polymer concentration. Therefore, we should not consider that the temperature dependence of the SEEPS-1/Oil-1 blends is due to the relaxation of individual chains.

Table 1 Activation energy of SEEPS-1/Oil-1 blends in the ordered state

100/0	75/25	50/50	25/75
(110 ± 10) kJ/mol	(120 ± 10) kJ/mol	(120 ± 10) kJ/mol	(120 ± 10) kJ/mol

We suppose that the temperature dependence (activation energy ΔE) of the viscoelastic properties of SEEPS-1/Oil-1 blends is due to the presence of defects of grain morphology. Koppi et al. (1992) proposed that the undulations and defects in the lamellar layers might contribute to the low-frequency viscoelastic behavior of block copolymers. Larson et al. (1993) also showed that the nonterminal behavior in block copolymers is caused by the existence of the lamellar structure with defects in the layers. They found that the low-frequency viscoelasticity of ordered block copolymers is very sensitive to grain network structure formed by continuity of the microdomains through the grain boundary region. If the temperature dependence of the viscoelasticity for the SEEPS-1/Oil-1 blends is attributed to effects of defects of microdomain structure and complicated grain boundaries, it should be independent of the type of microstructures (lamellae, cylinder, and sphere). Balsala et al. (1996) studied the effect grain size (or defect density) on the rheology of block copolymers and found that the rheological properties were not significantly affected by a change in the average grain size. The same ΔE values irrespective of blend ratio obtained here suggest that the temperature dependence of the viscoelastic response is due to the defects and grain boundary.

Concluding remarks

SAXS and low-frequency viscoelastic measurements were performed for the SEEPS-1/Oil-1 blends. The SAXS profiles indicated that the structures change from a lammelar microdomain to a hexagonally packed cylindrical microdomain of PS, and furthermore change to spherical microdomains packed in a cubic lattice with increasing oil content. SEEPS-1/Oil-1 = 100/0 and 75/25 blends held the same microdomain structure at elevating T below 300 °C investigated. However, SEEPS-1/Oil-1 = 50/50 and 25/75 blends exhibited ODT behavior. Corresponding to these SAXS observations below T_{ODT}, the viscoelastic properties exhibited characteristic features; the shear modulus is proportional to $\omega^{1/2}$, $\omega^{1/4 \sim 1/3}$, and ω^0 at low frequencies in locally lamellar, cylindrical, and spherical microdomains. The time-temperature superposition was applicable in the ordered state at low frequencies and the activation energy ΔE was roughly independent of blend composition (in other words, microdomain structure), suggesting that the temperature dependence of low frequency viscoelasticity is due to the presence of defects and grain boundary.

References

Bates FS (1984) Block copolymers near the microphase separation transition. 2. linear dynamic mechanical properties. Macromolecules 17: 2607–2613

Balsara NP, Dai HJ, Watanabe H, Sato T, Osaki K (1996) Influence of defect density on the rheology of ordered block copolymers. Macromolecules 29:3507–3510

Chung CI, Lin MI (1978) Nature of melt rheological transition in a styrene-butadiene-styrene block copolymer. J Polym Sci: Polym Phys Ed 16:545–553

Ferry JD (1980) Viscoelastic properties of polymers, 3rd edn. Wiley, New York

Floudas G, Ulrich R, Wiesner U (1999) Microphase separation in poly(-isoprene-b-ethylene oxide) diblock copolymer melts. 1. Phase state and kinetics of the order-to-order transition. J Chem Phys 110:652–662

Fredrikson GH, Bates FS (1996) Dynamics of block copolymers: theory and experiment. Annu Rev Mater Sci 26:501–550

Gouinlock EV, Porter RS (1977) Linear dynamic mechanical properties of an SBS block copolymer. Polym Eng Sci 17:534–543

Kawasaki K, Onuki A (1990) Dynamics and rheology of diblock copolymers quenched into microphase-separated states. Phys Rev A 42: 3664–3666

Koppi KA, Tirrell M, Bates FS, Almdal K, Colby RH (1992) Lamellae orientation in dynamically sheared diblock copolymer melts. J Phys II (France) 2:1941–1961

Koppi KA, Tirrell M, Bates FS, Almdal K, Mortensen K (1994) Epitaxial growth and shearing of the body centered cubic phase in diblock copolymer melts. J Rheol 38:999–1027

Kossuth MB, Morse DC, Bates FS (1999) Viscoelastic behavior of cubic phases in block copolymer melts. J Rheol 43:167–196

Larson RG, Winey KI, Patel SS, Watanabe H, Bruinsma R (1993) The rheology of layered liquids: lammelar block copolymers and smectic liquid crystals. Rheol Acta 32:245–253

Larson RG (1999) The structure and rheology of complex fluids. Oxford University Press, New York

Morrison FA, Winter HH (1989) Effect of unidirectional shear on the structure of triblock copolymers. 1. Polystyrene-polybutadiene-polystyrene. Macromolecules 22:3533–3540

Morrison FA, Winter HH, Gronski W, Barnes JD (1990) Effect of unidirectional shear on the structure of triblock copolymers. 2. polystyrene-polyisoprene-polystyrene. Macromolecules 23:4200–4205

Mortensen K, Almdal K, Kleppinger R, Mischenko N, Reynaers H (1998) Networks of gel-forming triblock copolymers solutions: in situ SANS and rheological measurements. Physica B 241-243: 1025–1028

Mortensen K, Theunissen E, Kleppinger R, Almdal K, Reynaers H (2002) Shear-induced morphologies of cubic ordered block copolymer micellar networks studied by in situ small-angle neutron scattering and rheology. Macromolecules 35:7773–7781

Nishioka A, Aoki Y, Suzuki T, Ishigami A, Endo T, Koda T, Koyama K (2011) Dynamic mechanical properties of polystyrene-block-poly[ethylene-co-(ethylene-propylene)]-block polystylene triblock copolymer/hydrocarbon oil blends. J Appl Polym Sci 121:3001–3006

Patel SS, Larson RG, Winey KI, Watanabe H (1995) Shear orientation and rheology of a lamellar polystyrene-polyisoprene block copolymer. Macromolecules 28:4313–4318

Rosedale JH, Bates FS (1990) Rheology of ordered and disordered symmetric poly(ethylenepropylene)-poly(ethylethylne) diblock copolymers. Macromolecules 23:2329–2338

Rubinstein M, Obukhov SP (1993) Power-law-like stress relaxation of block copolymers: disentanglement regimes. Macromolecules 26: 1740–1750

Ryu CY, Lee MS, Hajduk DA, Lodge TP (1997) Structure and viscoelasticity of matched asymmetric diblock and triblock copolymers in the cylinder and sphere microstructures. J Polym Sci Part B: Polym Phys 35:2811–2823

Sakamoto N, Hashimoto T, Han CD, Kim D, Vaidya NY (1997) Effect of addition of a neutral solvent on the order-order and order-disorder

transitions in a polystyrene-block-polyisoprene-block-polystyrene copolymer. Macromolecules 30:5321–5330

Sugimoto M, Sakai K, Aoki Y, Taniguchi T, Koyama K (2009) Rheology and morphology change with temperature of SEBS/hydrocarbon oil blends. J Polym Sci Part B: Polym Phys 47:955–965

Takahashi R, Nishioka A, Ishigami A, Suzuki T, Nishitsuji S, Koda T, Aoki Y (2012) Rheology of polystyrene-block-poly[ethylene-co-(ethylene-propylene)]- block-polystyrene triblock copolymer/ paraffinic oil blends - effect of oil molecular weight on the order-disorder transition -. Nihon Reoroji Gakkaishi (J Soc Rheol Jpn) 40: 171–177

Wang H, Newstein MC, Krishnan A, Balsara NP, Garetz BA, Hammouda B, Krishnamoorti R (1999) Ordering kinetics and alignment of block copolymer lamellae under shear flow. Macromolecules 32: 3639–3711

Watanabe H, Kotaka T, Hashimoto T, Shibayama M, Kawai H (1982) Rheological and morphological behavior of styrene-butadiene diblock copolymer solutions in selective solvents. J Rheol 26:153–179

Winter HH, Scott DB, Gronski W, Okamoto S, Hashimoto T (1993) Ordering by flow near the disorder-order transition of a triblock co-polymer styrene-isoprene-styrene. Macromolecules 26:7236–7244